Fluid mechanics of microchannel reactors for synthesis gas production

Junjie Chen

Department of Energy and Power Engineering, School of Mechanical and Power Engineering, Henan Polytechnic University, Jiaozuo, Henan, 454000, P.R. China

Corresponding author, E-mail address: cjjtpj@163.com

Abstract

The present study is focused primarily upon the fluid mechanics of microchannel reactors for synthesis gas production. The effect of surface features on the reactor performance is explored for the steam reforming reaction. The conversion rate is used to compare the reactor performance of different configurations. For the purpose of comparison, a baseline case is modeled which is a straight channel of the same dimensions as those for the cases with surface features in terms of channel length, channel width, and gap size. The reactor performance with surface features is quantitatively measured using different enhancement factors. The results indicate that the surface features are preferably at oblique angles, neither parallel nor perpendicular to the direction of net flow past a surface. Flow boiling can achieve very high convective heat transfer coefficients, and that coupled with the isothermal fluid allows the heat transfer wall to remain at quasi-constant temperature along the flow direction. Due to the existence of vapor slugs, severe flow and pressure oscillation may occur in microchannel boiling. Critical heat flux occurs when the temperature difference reaches a point where the heat transfer rate changes from nucleate and bubbly flow to local dry out and gas phase resistance starts to dominate heat transfer. As the momentum is increased at higher Reynolds numbers, the relative vorticity or angular force to spin the fluid also increases and thus the number of contacts or collisions with or near the active surface feature walls is also increased. The performance enhancement of the active surface features relative to a corresponding featureless or flat or smooth wall is typically improved as the residence time is decreased.

Keywords: Fluid mechanics; Microchannel reactors; Surface features; Synthesis gas; Catalyst deactivation; Energy efficiency

1. Introduction

A synthesis gas product is a product comprising primarily carbon monoxide and hydrogen. Reformed hydrocarbons may be further reacted in one or more shift reactors to form additional hydrogen in the process stream and separated in a separation unit, such as a pressure swing adsorption unit, to form a hydrogen product [1, 2]. Synthesis gas is conventionally used to produce synthesis gas products such as synthetic crude, or further upgraded to form intermediate or end products [3, 4]. The synthesis gas may also be used to produce one or more oxygenates, for example, ethers and alcohols. Synthesis gas can be produced from methane-containing feedstocks by any number of primary synthesis gas generation reactors [5, 6]. For example, synthesis gas can be produced in a steam methane reformer, an endothermic reactor where reaction is carried out either in heat exchange reactors, or by other means where substantial heat may be transferred to the reacting fluid, such as in the case of autothermal reforming, where a portion of the feedstock is combusted inside the reactor to provide heat for steam reforming either subsequently or in the same location as the combustion [7, 8]. Synthesis gas can also be produced from methane-containing feedstocks by dry reforming, catalytic or thermal partial oxidation and other processes.

Various feedstocks can be used to produce synthesis gas and industry desires to process multiple

feedstocks [9, 10]. Industry desires the ability to change from one feedstock to another during operation without shutting down the reactor [11, 12]. For example, a synthesis gas producer may desire to use natural gas for six months, naphtha for three months, and then a mixture of natural gas and naphtha for two months [13, 14]. Industry desires to process different feedstocks at optimal energy efficiency while avoiding carbon formation in the primary synthesis gas reactor [15, 16]. In addition to being able to process multiple feedstocks, industry desires to be able to process a feedstock where the composition, particularly the light hydrocarbon concentration in the feedstock, varies over time [17, 18]. For example, synthesis gas may be produced from a refinery off-gas where the light hydrocarbon concentration varies depending upon the refinery operation [19, 20]. If the feedstock contains higher hydrocarbons than methane, that is, hydrocarbons having two or more carbon atoms are used in the steam reforming process, the risk for catalyst deactivation by carbon deposition in the primary synthesis gas generation reactor is increased [21, 22]. Industry desires to avoid carbon formation in the synthesis gas generation reactor.

In order to reduce the risk of carbon deposition in the primary synthesis gas generation reactor, hydrogen and synthesis gas production processes may employ at least one catalytic reactor prior to the primary synthesis gas generation reactor where the catalytic reactor is operated at conditions less prone to hydrocarbon cracking than the primary synthesis gas generation reactor [23, 24]. These reactors positioned before the primary synthesis gas generation reactors are referred to as pre-reformers [25, 26]. Pre-reformers can be operated adiabatically or convectively heated by indirect heat transfer with combustion products gases from the primary synthesis gas generation reactor [27, 28]. The activity of the catalyst in the pre-reformer may degrade with use. Industry desires to compensate for the degradation of the pre-reforming catalyst through operational changes to avoid carbon formation in the primary synthesis gas generation reactor while maintaining optimal energy efficiency of the overall process [29, 30]. In hydrogen and synthesis gas production processes employing pre-reformers and steam methane reformers, the hydrocarbon feedstock may be mixed with hydrogen for a resultant stream having one to five percent hydrogen by volume, and subsequently subjected to a hydrodesulphurization pretreatment to remove Sulphur [31, 32]. The hydrocarbon feedstock may also be treated to remove olefins in a hydrogenation reactor. In case hydrogen is present in the feedstock, additional hydrogen might not be added [33, 34]. For steam reforming of heavy naphtha, hydrogen concentrations as high as about 50 percent by volume of hydrogen are known where the mixture is subsequently pretreated in a hydrodesulphurization unit and a hydrogenation reactor [35, 36]. Even higher hydrogen concentrations are possible depending on the feedstock provided.

The feedstock, after pretreating, is combined with superheated steam to form mixed feed having a prescribed steam-to-carbon molar ratio [37, 38]. The steam-to-carbon molar ratio is the ratio of the molar flow rate of steam in the mixed feed to the molar flow rate of hydrocarbon-based carbon in the mixed feed. The steam-to-carbon molar ratio for steam methane reforming of natural gas typically ranges from 2 to 5, but can be as low as 1.5. The steam-to-carbon molar ratio is generally higher for steam methane reforming of feedstock containing a greater number of higher hydrocarbons, for example, propane, butane, propane and butane mixtures, and naphtha. Higher steam flow rates are used to suppress carbon formation and enhance the steam reforming reaction. However, higher steam-to-carbon molar ratios disadvantageously decrease the energy efficiency of the reforming process. Industry desires to improve the energy efficiency of steam-hydrocarbon reforming systems [39, 40]. A significant disadvantage which inhibits the wider use of fuel cells is the lack of a widespread hydrogen infrastructure. Hydrogen has a relatively low volumetric efficiency and is more difficult to store and transport than the hydrocarbon fuels currently used in most power generation systems. One way to overcome this difficulty is the use of reformers to convert the hydrocarbons to a hydrogen-rich gas stream that can be used as a feed for fuel cells [41, 42]. Fuel reforming processes, such as steam

reforming, partial oxidation, and autothermal reforming, can be used to convert hydrocarbon fuels into a hydrogen rich gas. In addition to the desired product hydrogen, undesirable byproduct compounds such as carbon dioxide and carbon monoxide are found in the product gas. For many uses, such as fuel for proton exchange membrane or alkaline fuel cells, these contaminants reduce the value of the product gas in part due to the sensitivity of proton exchange membrane fuel cells to carbon monoxide and sulfur [43, 44]. In a conventional steam reforming process, a hydrocarbon feed is vaporized, mixed with steam, and passed over a steam reforming catalyst. The majority of the feed hydrocarbon is converted to a mixture of hydrogen, carbon monoxide, and carbon dioxide. The reforming product gas is typically fed to a water-gas shift bed in which much of the carbon monoxide is reacted with steam to form carbon dioxide and hydrogen [45, 46]. However, water-gas shift beds tend to be large complex units that are typically sensitive to air, further complicating their startup and operation.

The present study is focused primarily upon the method and apparatus for steam reforming methanol. Carbon monoxide, carbon dioxide and mixtures thereof, can be removed from the hydrogen-rich reformate by subjecting the hydrogen-rich reformate to one or more of a water gas shift reaction, methanation, and selective oxidation. The present design provides a method of generating electricity comprising the steps of reducing the sulfur content of the sulfur-containing hydrocarbon fuel, catalytically converting the reduced-sulfur hydrocarbon fuel to hydrocarbons, steam reforming the mixture of hydrocarbons at a steam reforming temperature in a catalyst bed to produce a reformate comprising hydrogen and carbon dioxide, fixing at least a portion of the carbon dioxide in the reformate with a carbon dioxide fixing material in the catalyst bed to produce a hydrogen-rich reformate, and feeding the hydrogen-rich reformate to an anode of a fuel cell, wherein the fuel cell consumes a portion of the hydrogen rich reformate and produces electricity, an anode tail gas and a cathode tail gas. The method can further include the step of feeding at least a portion of the tail gases to a combustor or anode tail gas oxidizer to produce an exhaust gas for use in the steam reforming of sulfur-containing hydrocarbon fuels. Optionally, but preferably, the method further includes the step of reducing the amount of carbon monoxide and carbon dioxide in the hydrogen-rich reformate by subjecting the hydrogen-rich reformate to one or more of a water gas shift reaction, methanation and selective oxidation. An integrated system in which tail gas from the fuel cell and hydrogen storage system is used to provide heat needed to reform the feed fuel and regenerate the calcium oxide bed. This study aims to feed the hydrogen-rich reformate to an anode of a fuel cell, wherein the fuel cell consumes a portion of the hydrogen-rich reformate and produces electricity, an anode tail gas, and a cathode tail gas. Particular emphasis is placed upon a fuel cell configured to receive the hydrogen-rich reformate from the fuel processor and wherein the fuel cell consumes a portion of the hydrogen-rich reformate and produces electricity, an anode tail gas, and a cathode tail gas.

2. Methods

The microchannel reactor is illustrated schematically in Figure 1 for the steam reforming process. A catalytic reaction channel is a channel containing a catalyst, where the catalyst may be heterogeneous or homogeneous. A homogeneous catalyst may be co-flowing with the reactants. Microchannel apparatus is similarly characterized, except that a catalyst-containing reaction channel is not required. The sides of a microchannel are defined by reaction channel walls. These walls are preferably made of a hard material such as a ceramic, an iron-based alloy such as steel, or a Ni-based, Co-based, or Fe-based superalloy [47, 48]. They also may be made from plastic, glass, or other metal such as copper, aluminum and the like. The choice of material for the walls of the reaction channel may depend on the reaction for which the reactor is intended. In some cases, reaction chamber walls are comprised of a stainless steel or Inconel® which is durable and has good thermal conductivity [49, 50]. The alloys should be low in sulfur, and in some cases are subjected to a desulfurization treatment prior to

formation of an aluminide. Typically, reaction channel walls are formed of the material that provides the primary structural support for the microchannel apparatus. Microchannel apparatus can be made by known methods, and in some cases are made by laminating interleaved plates, and preferably where shims designed for reaction channels are interleaved with shims designed for heat exchange. Some microchannel apparatus includes at least 10 layers laminated in a device, where each of these layers contain at least 10 channels; the device may contain other layers with less channels.

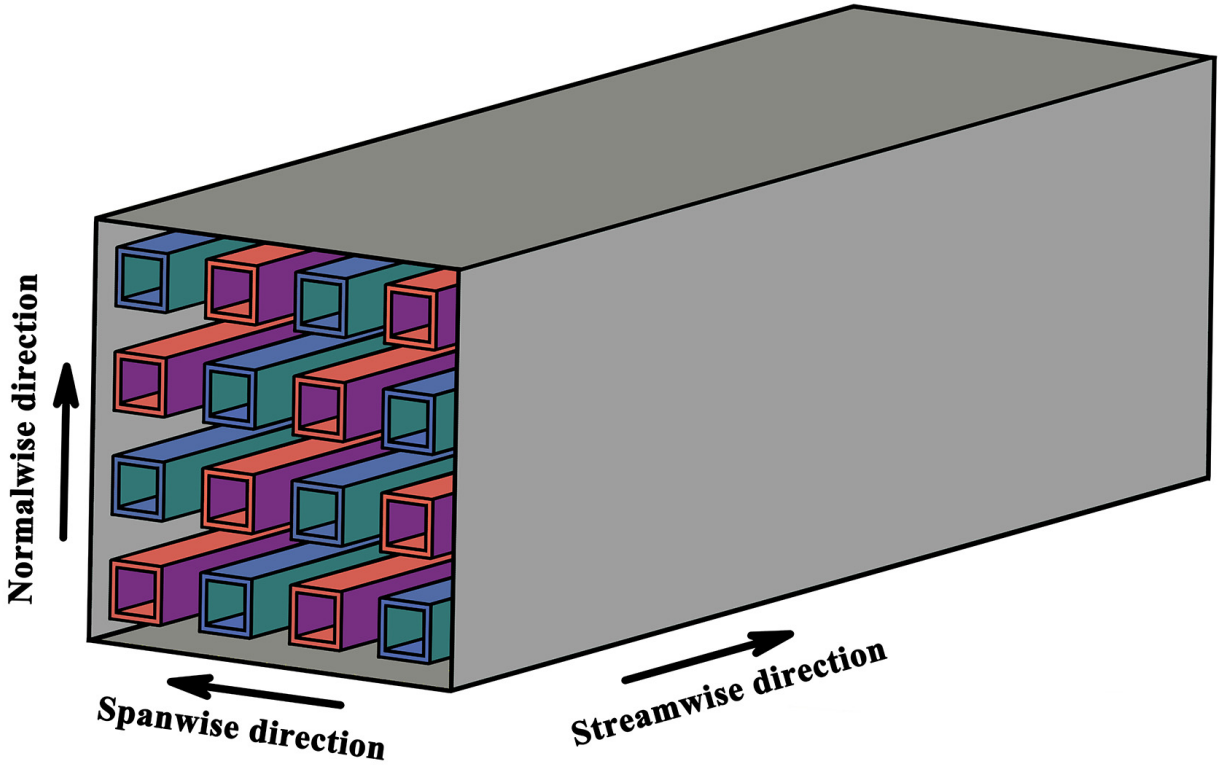

Figure 1. Physical representation of the microchannel reactor for the steam reforming process in which tail gas from the fuel cell and hydrogen storage system is used to provide heat needed to reform the feed fuel and regenerate the calcium oxide bed.

Microchannel reactors preferably include microchannels and a plurality of adjacent heat exchange microchannels. The adjacent heat exchange microchannels are illustrated schematically in Figure 2 in which contact time is maintained about constant but the length of each stage increases progressively to accommodate the higher flow rate in each stage. Each stage can have the same length or stages can have different lengths. The plurality of microchannels may contain, for example, 2, 10, 100, 1000 or more channels capable of operating in parallel. In preferred cases, the microchannels are arranged in parallel arrays of planar microchannels, for example, at least 3 arrays of planar microchannels. Performance advantages in the use of this type of reactor architecture for the purposes of the present design include their relatively large heat and mass transfer rates, and the substantial absence of any explosive limits [51, 52]. Pressure drops can be low, allowing high throughput and the catalyst can be fixed in a very accessible form within the channels eliminating the need for separation. In some cases, a reaction microchannel contains a bulk flow path. The term bulk flow path refers to an open path within the reaction chamber. A contiguous bulk flow region allows rapid fluid flow through the reaction chamber without large pressure drops. In devices with multiple manifolds, the design can be characterized by the volume ratio of one manifold to its connecting microchannels, or characterized by the volumetric sum of plural manifolds and their connecting microchannels. However, if connecting channels are connected to a header and footer, then both the header and footer must be included in the calculation of manifold volume [53, 54]. The volume of the submanifold is included in the volume of the manifold. A general methodology to build commercial scale microchannel devices is to form the

microchannels in the shims by different methods such as etching and stamping [55, 56]. For example, shims may be stacked together and joined by different methods such as chemical bonding and brazing. After joining, the device may or may not require machining.

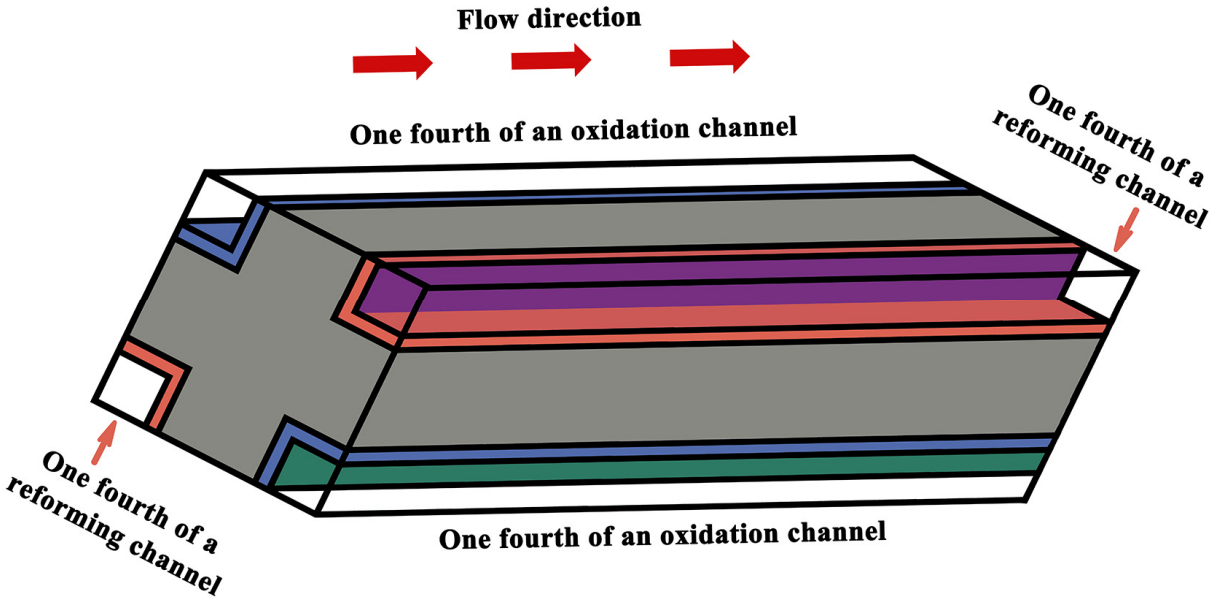

Figure 2. Physical representation of the adjacent heat exchange microchannels in which contact time is maintained about constant but the length of each stage increases progressively to accommodate the higher flow rate in each stage.

The law of conservation of mass is stated as

$$\frac{\partial(\rho u_x)}{\partial x}+\frac{\partial(\rho u_y)}{\partial y}+\frac{\partial(\rho u_z)}{\partial z}=0, \tag{1}$$

in which ρ denotes the density and u denotes the velocity.

The law of conservation of energy in the solid phase is stated as

$$\frac{\partial}{\partial x}\left(\lambda_w\frac{\partial T}{\partial x}\right)+\frac{\partial}{\partial y}\left(\lambda_w\frac{\partial T}{\partial y}\right)+\frac{\partial}{\partial z}\left(\lambda_w\frac{\partial T}{\partial z}\right)=0, \tag{2}$$

wherein λ is the thermal conductivity.

The law of conservation of energy in the gas phase is stated as

$$\begin{aligned}&\frac{\partial}{\partial x}\left(\rho\sum_{g=1}^{K_g}Y_g h_g V_{g,x}-\lambda_m\frac{\partial T}{\partial x}\right)+\frac{\partial}{\partial y}\left(\rho\sum_{g=1}^{K_g}Y_g h_g V_{g,y}-\lambda_m\frac{\partial T}{\partial y}\right)+\frac{\partial}{\partial z}\left(\rho\sum_{g=1}^{K_g}Y_g h_g V_{g,z}-\lambda_m\frac{\partial T}{\partial z}\right)\\&+\frac{\partial(\rho u_x h)}{\partial x}+\frac{\partial(\rho u_y h)}{\partial y}+\frac{\partial(\rho u_z h)}{\partial z}=0\end{aligned}, \tag{3}$$

$$\vec{V}_g=-D_g^m\nabla\left(\ln\left(\frac{Y_g M'}{M_g}\right)\right)+\left(\frac{D_g^T M_g}{\rho Y_g M'}\right)\nabla(\ln T), \tag{4}$$

in which T is the temperature, Y is the mass fraction, M is the molar mass, M' is the mean molar mass, V is the diffusion velocity, h is the enthalpy, and D^T and D^m are the thermal and molecular diffusivity.

The law of conservation of surface species is stated as

$$\frac{\theta_s\dot{s}_s}{\gamma}=0, \tag{5}$$

in which θ denotes the coverage, γ denotes the active site density, and $\dot{s}$ denotes the production rate.

The law of conservation of gas-phase species is stated as

$$\frac{\partial\left(\rho u_x Y_g\right)}{\partial x}+\frac{\partial\left(\rho u_y Y_g\right)}{\partial y}+\frac{\partial\left(\rho u_z Y_g\right)}{\partial z}+\frac{\partial}{\partial x}\left(\rho Y_g V_{g,x}\right)+\frac{\partial}{\partial y}\left(\rho Y_g V_{g,y}\right)+\frac{\partial}{\partial z}\left(\rho Y_g V_{g,z}\right)=0. \tag{6}$$

The law of conservation of momentum is stated as

$$\begin{aligned}&\frac{\partial}{\partial x}\left[\mu\left(\frac{\partial u_x}{\partial x}+\frac{\partial u_x}{\partial x}\right)\right]+\frac{\partial}{\partial y}\left[\mu\left(\frac{\partial u_x}{\partial y}+\frac{\partial u_y}{\partial x}\right)\right]+\frac{\partial}{\partial z}\left[\mu\left(\frac{\partial u_x}{\partial z}+\frac{\partial u_z}{\partial x}\right)\right]\\&-\frac{\partial}{\partial x}\left[\frac{2}{3}\mu\left(\frac{\partial u_{xx}}{\partial x}+\frac{\partial u_{yx}}{\partial y}+\frac{\partial u_{zx}}{\partial z}\right)\right]-\frac{\partial p}{\partial x}=0\end{aligned}, \tag{7}$$

$$\begin{aligned}&\frac{\partial}{\partial x}\left[\mu\left(\frac{\partial u_y}{\partial x}+\frac{\partial u_x}{\partial y}\right)\right]+\frac{\partial}{\partial y}\left[\mu\left(\frac{\partial u_y}{\partial y}+\frac{\partial u_y}{\partial y}\right)\right]+\frac{\partial}{\partial z}\left[\mu\left(\frac{\partial u_y}{\partial z}+\frac{\partial u_z}{\partial y}\right)\right]\\&-\frac{\partial}{\partial y}\left[\frac{2}{3}\mu\left(\frac{\partial u_{xy}}{\partial x}+\frac{\partial u_{yy}}{\partial y}+\frac{\partial u_{zy}}{\partial z}\right)\right]-\frac{\partial p}{\partial y}=0\end{aligned}, \tag{8}$$

$$\begin{aligned}&\frac{\partial}{\partial x}\left[\mu\left(\frac{\partial u_z}{\partial x}+\frac{\partial u_x}{\partial z}\right)\right]+\frac{\partial}{\partial y}\left[\mu\left(\frac{\partial u_z}{\partial y}+\frac{\partial u_y}{\partial z}\right)\right]+\frac{\partial}{\partial z}\left[\mu\left(\frac{\partial u_z}{\partial z}+\frac{\partial u_z}{\partial z}\right)\right]\\&-\frac{\partial}{\partial z}\left[\frac{2}{3}\mu\left(\frac{\partial u_{xz}}{\partial x}+\frac{\partial u_{yz}}{\partial y}+\frac{\partial u_{zz}}{\partial z}\right)\right]-\frac{\partial p}{\partial z}=0\end{aligned}, \tag{9}$$

wherein μ denotes the dynamic viscosity.

3. Results and discussion

The hydrogen mole fraction contour map in the reactor is plotted in Figure 3 wherein the leading edge of the subsurface layer has a tapered shape that corresponds to the angle of cross-bars in the top-most layer so that fluids from the bulk flow path are not trapped beneath the top-most layer. A hydraulic diameter of a channel is defined as four times the cross-sectional area of the channel divided by the length of the channel's wetted perimeter. A manifold is a volume that distributes flow to two or more connecting channels. The entrance, or inlet, surface of a header manifold is defined as the surface in which marks a significant difference in header manifold geometry from the upstream channel. The exit, or outlet, surface of the footer manifold is defined as the surface which marks a significant difference in the footer manifold channel from the downstream channel. For rectangular channels and most other typical manifold geometries, the surface will be a plane; however, in some special cases such as hemi-circles at the interface between the manifold and connecting channels it will be a curved surface. The value of the Reynolds number describes the flow regime of the stream. While the dependence of the regime on Reynolds number is a function of channel cross-section shape and size. The porous supports may be stacked between a heat transfer wall and a sheet with apertures. Alternatively, the porous supports may be etched, cut or otherwise have active surface feature grooves placed within the sheets. The sheets may be stacked with non-porous sheets that serve as walls to form an assembly. An active catalyst layer or layers may be disposed upon the large pore support. A surface feature is a projection from, or a recess into, a microchannel wall that modify flow within the microchannel. If the area at the top of the features is the same or exceeds the area at the base of the feature, then the feature may be considered recessed. If the area at the base of the feature exceeds the

area at the top of the feature, then it may be considered protruded. The surface features have a depth, a width, and a length for non-circular surface features. Surface features may include circles, oblong shapes, squares, rectangles, checks, chevrons, zig-zags, and the like, recessed into the wall of a main channel. The features increase surface area and create convective flow that brings fluids to a microchannel wall through advection rather than diffusion. Flow patterns may swirl, rotate, tumble and have other regular, irregular and or chaotic patterns, although the flow pattern is not required to be chaotic and, in some cases, may appear quite regular. The flow patterns are stable with time, although they may also undergo secondary transient rotations. The surface features are preferably at oblique angles, neither parallel nor perpendicular to the direction of net flow past a surface. Surface features may be orthogonal, that is at a 90-degree angle, to the direction of flow, but are preferably angled. The active surface features are further preferably defined by more than one angle along the width of the microchannel at least at one axial location. The two or more sides of the surface features may be physically connected or disconnected. The one or more angles along the width of the microchannel act to preferentially push and pull the fluid out of the straight laminar streamlines.

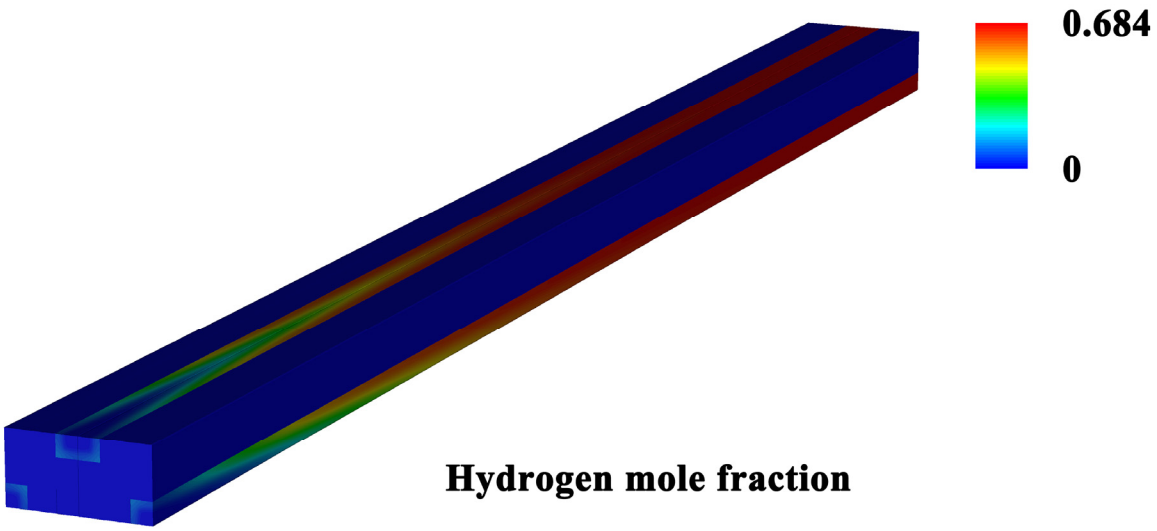

Figure 3. Hydrogen mole fraction contour map in the reactor wherein the leading edge of the subsurface layer has a tapered shape that corresponds to the angle of cross-bars in the top-most layer so that fluids from the bulk flow path are not trapped beneath the top-most layer.

The temperature contour map in the reactor is plotted in Figure 4 wherein the leading edge of the subsurface layer has a tapered shape that corresponds to the angle of cross-bars in the top-most layer so that fluids from the bulk flow path are not trapped beneath the top-most layer. For decades, steam reforming has been the principal industrial process for making hydrogen. More recently, steam reforming has attracted great interest as a possible means to supply hydrogen for fuel cells [57, 58]. There have been intensive research efforts over many years to improve the steam reforming process [59, 60]. Despite these efforts, problems continue to exist with catalyst performance and cost, and the need for catalyst replacement or regeneration due to the rather harsh conditions in which steam reforming is typically conducted. The volume of a connecting channel or manifold is based on open space. The volume includes depressions of surface features. The volume of gate or grate features, which help equalize flow distribution as described in the incorporated published patent application, are included in the volume of manifold; this is an exception to the rule that the dividing line between the manifold and the connecting channels is marked by a significant change in direction. Channel walls are not included in the volume calculation. Similarly, the volume of orifices, which is typically negligible, and flow straighteners are included in the volume of manifold. Boiling is known as a highly efficient heat transfer mechanism that provides high heat flux density based on surface area and volume. There are

several different boiling regimes including low vapor quality flow, nucleate boiling, film boiling and transition boiling. Nucleate boiling is mostly found in the industrial applications. Boiling can take place at heat transfer surface both in fluid flow and fluid pool or in the volume of the fluid. Through phase change of the fluid, flow boiling has the potential to achieve an isothermal heat sink in the fluid while the phase change is occurring. Flow boiling can achieve very high convective heat transfer coefficients, and that coupled with the isothermal fluid allows the heat transfer wall to remain at quasi-constant temperature along the flow direction. This is a desirable heat transfer situation for many thermal, nuclear and chemical process applications. In many chemical processes, such as an exothermic chemical reactor, the reaction rate strongly depends on the local temperature. An optimal temperature throughout the reaction zone often leads to a maximum yield, conversion and desired selectivity. Thus, boiling heat transfer is used in process control or thermal management of various reactions to maintain an isothermal thermal condition where the exothermic reactions releases heat. Compared to a boiling process control, a cooling system via single-phase fluid convection generally cannot achieve a near isothermal boundary condition for the reactions without large flow rates needed to keep the stream at constant temperatures and increase the convective heat flux.

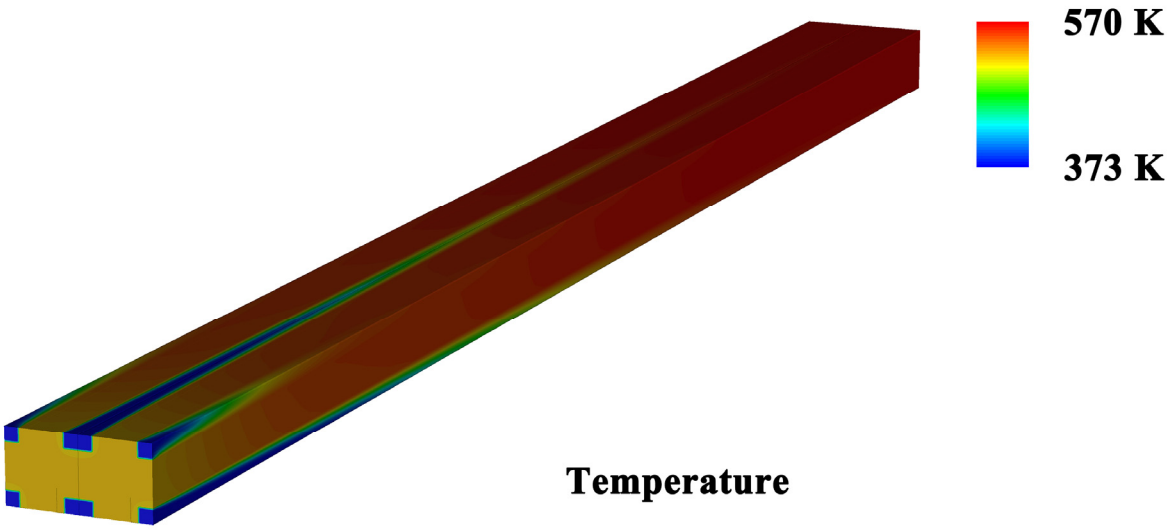

Figure 4. Temperature contour map in the reactor wherein the leading edge of the subsurface layer has a tapered shape that corresponds to the angle of cross-bars in the top-most layer so that fluids from the bulk flow path are not trapped beneath the top-most layer.

The sensible enthalpy contour map in the reactor is plotted in Figure 5 wherein the leading edge of the subsurface layer has a tapered shape that corresponds to the angle of cross-bars in the top-most layer so that fluids from the bulk flow path are not trapped beneath the top-most layer. So far, boiling in microchannels has not been used in the thermal management and control of the microchannel chemical reaction processes due to various postulated or practical technical issues. Flow boiling in microchannels is associated with the flow patterns different from that found in the ordinary flow channels where vapor bubbles are smaller than the channel diameters and the channel wall is generally well wetted by the liquid. The hydraulic diameter of microchannels is usually smaller than the characteristic diameter of the vapor bubbles so that due to capillary effect vapor slugs and liquid slugs consecutively flow by a fixed location of the channel. The prediction methods and design criteria for this flow pattern are not well established. The other desired flow patterns such as bubbly flow and annular flow may only be possible in a very narrow flow parameter range or limited operation conditions or may be absent. Due to the existence of vapor slugs, local hot spot of the wall and in turn the temperature non-uniformity may occur due to the low vapor-wall heat transfer rate. Due to the existence of vapor slugs, severe flow and pressure oscillation may occur in microchannel boiling. Instability of the entire cooling system may

instantly occur. The heat transfer crisis can occur even at low heat duty due to the large difference between the heat transfer coefficients by evaporation and by single-phase vapor convection. This is characterized by the critical heat flux that may be very low and lead to non-isothermal heat transfer. The flow distribution and manifolding are difficult in microchannel arrays with two-phase flow, while a large number of integrated microchannels is usually needed for the desired process capacity. The present process makes it possible to make use of flow boiling in microchannels integrated in unit operations to realize a stable isothermal boundary condition for the exothermal reaction. The reaction process can be thus thermally controlled to operate in an optimal condition. The local quality of the convicting flow is needed to estimate the pressure drop in a channel. Knowing the void fraction and vapor quality variation along the channel length, the two-phase pressure drop in the channel can be calculated using a separated flow model. The term critical heat flux is the local heat flux at which wall temperature cannot be maintained due to heat transfer mechanism change from boiling to vapor convection. This results in the formation of a localized hot spot.

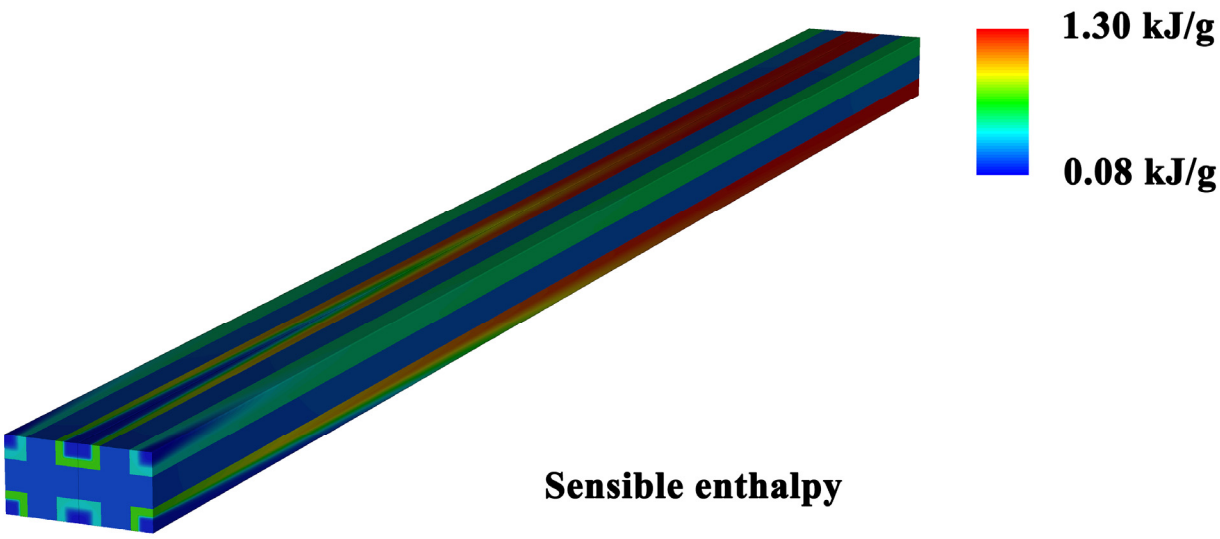

Figure 5. Sensible enthalpy contour map in the reactor wherein the leading edge of the subsurface layer has a tapered shape that corresponds to the angle of cross-bars in the top-most layer so that fluids from the bulk flow path are not trapped beneath the top-most layer.

The enthalpy contour map in the reactor is plotted in Figure 6 wherein the leading edge of the subsurface layer has a tapered shape that corresponds to the angle of cross-bars in the top-most layer so that fluids from the bulk flow path are not trapped beneath the top-most layer. Smaller values of the temperature difference range have single phase heat transfer and low heat fluxes. There is a threshold temperature difference where nucleate boiling starts and increasing the difference slightly can result in larger heat fluxes, as nucleate boiling starts to occur. Critical heat flux occurs when the temperature difference reaches a point where the heat transfer rate changes from nucleate and bubbly flow to local dry out and gas phase resistance starts to dominate heat transfer. Critical heat flux can occur before dry-out. Critical heat flux results in larger hydraulic diameters are fairly well characterized. Channel size and vapor quality are related to average wall heat flux in saturated boiling [61, 62]. Consequently, higher process heat flux quickly approaches local critical heat flux via higher vapor generation rate and accumulated vapor amount. The difference between the wall temperature and the saturation temperature is defined as the overage temperature. For a matrix of aligned microchannels where the local heat flux varies from channel to channel the difficulties described above become more challenging. Potential unit operations that would have a varying heat flux profile over a matrix of connecting channels include but aren't limited to the following factors: Exothermic chemical reactions, catalytic or homogeneous, distillation tower heat removal, desorption stage in an absorption or adsorption system, exothermic

mixing processes, and the like. This can occur when the microchannels are aligned cross-flow to the direction of the other unit operation's channels. For the varying channel flux situation there may be need for more flow in channels with the higher heat fluxes and less flow to channels with less heat fluxes to sustain convective boiling. It should be noted that from a heat transfer performance standpoint, isolated bubbles are most desirable. The catalyst may be supported on a porous support structure such as a foam, felt, wad or a combination thereof. The term foam is used herein to refer to a structure with continuous walls defining pores throughout the structure. The term felt is used herein to refer to a structure of fibers with interstitial spaces therebetween. The term wad is used herein to refer to a structure of tangled strands, like steel wool. The catalyst may be supported on a honeycomb structure. The catalyst may be supported on a flow-by support structure such as a felt with an adjacent gap, a foam with an adjacent gap, a fin structure with gaps, a wash-coat on any inserted substrate, or a gauze that is parallel to the flow direction with a corresponding gap for flow.

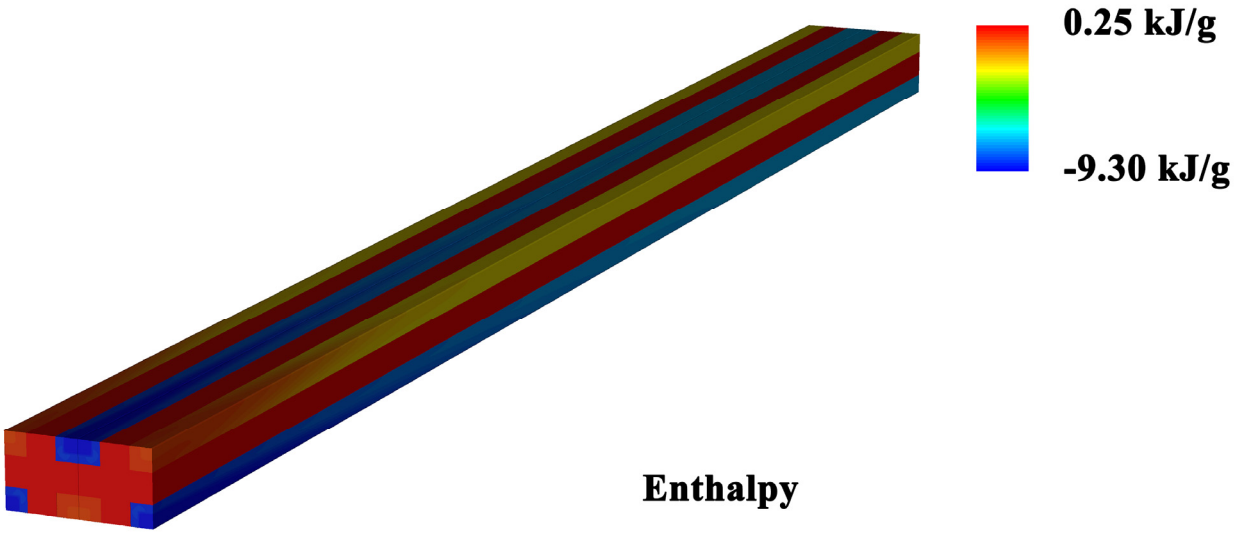

Figure 6. Enthalpy contour map in the reactor wherein the leading edge of the subsurface layer has a tapered shape that corresponds to the angle of cross-bars in the top-most layer so that fluids from the bulk flow path are not trapped beneath the top-most layer.

The methanol conversion results are presented in Figure 7 for the reactor wherein the volume occupied by the catalyst supported on a mesoporous matrix plus the volume of bulk flow path that is adjacent to the catalyst supported on a mesoporous matrix defines the volume of reaction chamber. All microchannel experiments are conducted with a certain fixed geometry. For the purposes of summarizing heat transfer performance for these devices, the length-to-diameter ratio, typically the channel length divided by the hydraulic diameter is a very useful metric [63, 64]. Boiling heat transfer characteristics of a microchannel can also be enhanced by applying a porous coating or in some means engineer porous or grooved structures on the wall surfaces of a microchannel. For unit operations, including homogeneous chemical reactions and heat exchangers, interaction of the bulk flow species with the active surface feature wall is advantageous to transfer heat to an adjacent heat transfer chamber. Unlike the prior micromixers, it is desirable to move the bulk stream near and past the wall and not necessarily completely and uniformly mix the bulk flow stream. An active surface feature wall that moves more fresh fluid near and past the active surface will be preferential over a design that primarily mixes the bulk stream. For these applications, performance is enhanced with higher Reynolds numbers as opposed to disadvantaged at higher Reynolds numbers because the high momentum streams are moved into a repeating rotating flow pattern that winds the bulk flow past the active surface features and does not substantially stop the flow rotation and try to turn it back in an opposing direction. Once the flow has started to turn in a fixed direction within the active surface features, it continues in the

same direction thus demonstrating a high vorticity such that the fluid is replenished against the active surface feature walls. As the momentum is increased at higher Reynolds numbers, the relative vorticity or angular force to spin the fluid also increases and thus the number of contacts or collisions with or near the active surface feature walls is also increased. For these cases, however, vorticity alone is not the only element [65, 66]. Patterns that merely spin the fluid in the bulk flow path, such as that created by a single angular diagonal feature groove across the width of a microchannel wall do not do a good job of pulling the center flow stream into the active surface features. In the present invention, the geometry of the active surface feature wall pattern may be designed to enhance contact, as defined to a molecule breaking the plane of the active surface feature groove and entering into the recessed and angled groove, with active surface features. The preferable active surface features have more than one angle across the width of at least one wall of the microchannel. The feature is preferably contiguous such as a chevron or zig-zag; but in some embodiments a surface feature having at least one angle could be discontinuous if the elements of the feature are aligned so that, except for a gap, the recesses or protrusions would connect, an example is a chevron with a missing apex. The catalyst may be directly wash-coated on the interior walls of the process microchannels, grown on the walls from solution, or coated in situ on a fin structure. The catalyst may be in the form of a single piece of porous contiguous material, or many pieces in physical contact. The catalyst may be comprised of a contiguous material and has a contiguous porosity such that molecules can diffuse through the catalyst. The catalyst may comprise a porous support, an interfacial layer on the porous support, and a catalyst material on the interfacial layer. The interfacial layer may be solution deposited on the support or it may be deposited by chemical vapor deposition or physical vapor deposition.

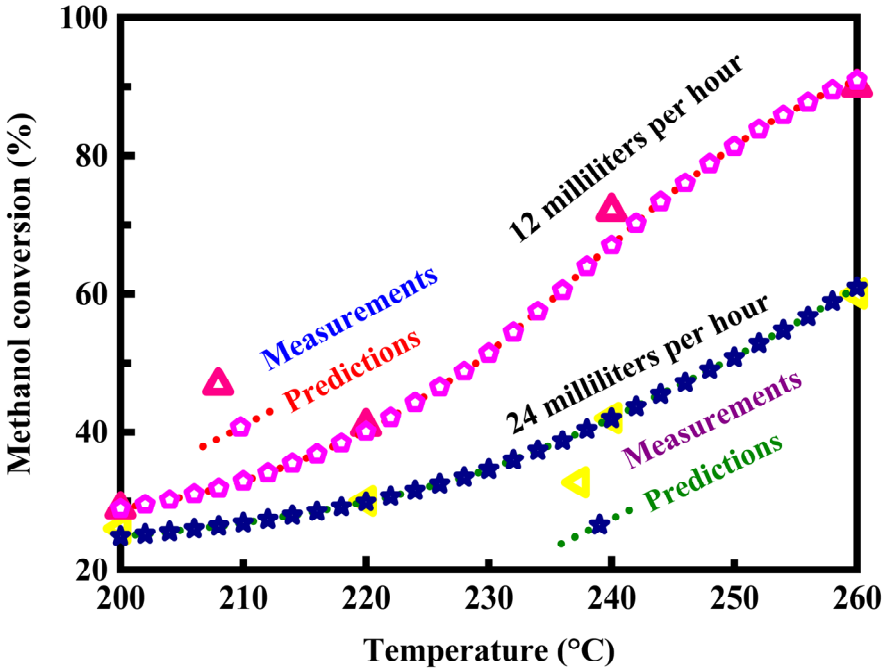

Figure 7. Methanol conversion of the reactor wherein the volume occupied by the catalyst supported on a mesoporous matrix plus the volume of bulk flow path that is adjacent to the catalyst supported on a mesoporous matrix defines the volume of reaction chamber.

The hydrogen productivity results are presented in Figure 8 for the reactor wherein the volume occupied by the catalyst supported on a mesoporous matrix plus the volume of bulk flow path that is adjacent to the catalyst supported on a mesoporous matrix defines the volume of reaction chamber. The performance enhancement of the active surface features relative to a corresponding featureless or flat or smooth wall is typically improved as the residence time is decreased. The featureless wall is defined by a microchannel that has a gap not inclusive of the depth of the recessed features and having the same

width and length. As the Reynolds number increases the importance of inertial forces increases. For higher inertia or momentum streams, maintaining the momentum in a single primary direction rather than reversing or changing directions makes it easier to keep the stream turning. As the stream keeps turning, it keeps moving more and more flow or molecules into the active surface features where they may interact with the walls that exchange either heat or mass or both. Mass of fluid entering a surface feature is defined as the amount of mass at the inlet to a surface feature section that enters at least one surface feature in a surface feature section, wherein entering a surface feature means the fluid molecule breaks the plane of the recessed surface feature and moves out of the bulk flow channel. Computational fluid dynamics code should be used to evaluate the percentage of mass that enters at least one surface feature in a surface feature section, which allows the evaluation of the fluid flow path lines to be illustrated and traced through the surface feature section. The surface feature section should be discretized with a minimum of six volume cells in the depth and length directions to get reasonable flow discretization, with the main straight channel discretized with proportionally sized cells to maintain the cell size continuity in the channel adjacent to the surface features and the spaces between the surface features. The Reynolds number is the commonly used ratio of the inertial over the viscous forces seen by flow in a channel. Its definition is the ratio of the mass flux rate times the hydraulic diameter divided by the dynamic viscosity. Coatings could also be applied onto microchannel walls by filling channels to the desired height with a liquid coating composition and removing volatile components under reduced pressure. Care may need to be exercised to avoid bubbling defects. The effect of surface features on the reactor performance is explored for the steam reforming reaction. The intent of the features is to increase the conversion per length, especially at low catalyst activity. The surface features increase the available surface area for catalyst, they allow a solution derived catalyst to be wash-coated uniformly, and they reduce external mass transport limitations in the bulk microchannel and thus allow the reactor to operate closer to the intrinsic potential of the catalyst activity.

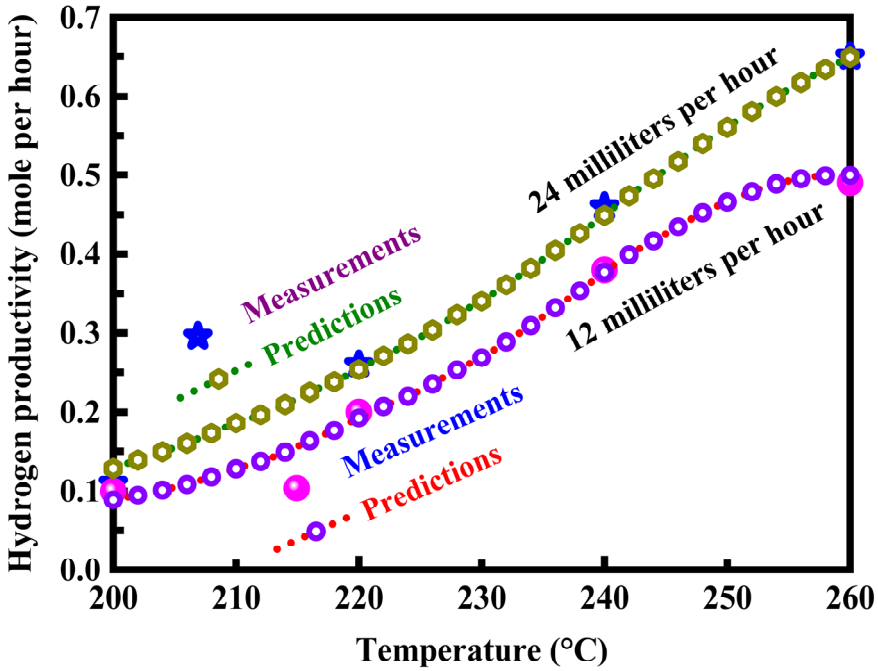

Figure 8. Hydrogen productivity of the reactor wherein the volume occupied by the catalyst supported on a mesoporous matrix plus the volume of bulk flow path that is adjacent to the catalyst supported on a mesoporous matrix defines the volume of reaction chamber.

4. Conclusions

The effect of surface features on the reactor performance is explored for the steam reforming

reaction. The conversion rate is used to compare the reactor performance of different configurations. For the purpose of comparison, a baseline case is modeled which is a straight channel of the same dimensions as those for the cases with surface features in terms of channel length, channel width, and gap size. The reactor performance with surface features is quantitatively measured using different enhancement factors. The major conclusions are summarized as follows:

- The surface features are preferably at oblique angles, neither parallel nor perpendicular to the direction of net flow past a surface.
- Flow boiling can achieve very high convective heat transfer coefficients, and that coupled with the isothermal fluid allows the heat transfer wall to remain at quasi-constant temperature along the flow direction.
- Due to the existence of vapor slugs, severe flow and pressure oscillation may occur in microchannel boiling.
- Critical heat flux occurs when the temperature difference reaches a point where the heat transfer rate changes from nucleate and bubbly flow to local dry out and gas phase resistance starts to dominate heat transfer.
- As the momentum is increased at higher Reynolds numbers, the relative vorticity or angular force to spin the fluid also increases and thus the number of contacts or collisions with or near the active surface feature walls is also increased.
- The performance enhancement of the active surface features relative to a corresponding featureless or flat or smooth wall is typically improved as the residence time is decreased.

References

[1] H.C. Yoon, J. Otero, and P.A. Erickson. Reactor design limitations for the steam reforming of methanol. *Applied Catalysis B: Environmental*, Volume 75, Issues 3-4, 2007, Pages 264-271.

[2] F. Soyal-Baltacıoğlu, A.E. Aksoylu, and Z.I. Önsan. Steam reforming of ethanol over Pt-Ni Catalysts. *Catalysis Today*, Volume 138, Issues 3-4, 2008, Pages 183-186.

[3] L. Shi, D.J. Bayless, and M. Prudich. A model of steam reforming of iso-octane: The effect of thermal boundary conditions on hydrogen production and reactor temperature. *International Journal of Hydrogen Energy*, Volume 33, Issue 17, 2008, Pages 4577-4585.

[4] J.A. Medrano, M. Oliva, J. Ruiz, L. Garcia, and J. Arauzo. Catalytic steam reforming of acetic acid in a fluidized bed reactor with oxygen addition. *International Journal of Hydrogen Energy*, Volume 33, Issue 16, 2008, Pages 4387-4396.

[5] A. Basile, F. Gallucci, and L. Paturzo. Hydrogen production from methanol by oxidative steam reforming carried out in a membrane reactor. *Catalysis Today*, Volume 104, Issues 2-4, 2005, Pages 251-259.

[6] A. Karim, J. Bravo, and A. Datye. Nonisothermality in packed bed reactors for steam reforming of methanol. *Applied Catalysis A: General*, Volume 282, Issues 1-2, 2005, Pages 101-109.

[7] F. Melo and N. Morlanés, Naphtha steam reforming for hydrogen production. *Catalysis Today*, Volumes 107-108, 2005, Pages 458-466.

[8] A. Olivieri and F. Vegliò. Process simulation of natural gas steam reforming: Fuel distribution optimisation in the furnace. *Fuel Processing Technology*, Volume 89, Issue 6, 2008, Pages 622-632.

[9] S. Lee, J. Bae, S. Lim, and J. Park. Improved configuration of supported nickel catalysts in a steam reformer for effective hydrogen production from methane. *Journal of Power Sources*, Volume 180, Issue 1, 2008, Pages 506-515.

[10] P.O. Graf, B.L. Mojet, J.G.V. Ommen, and L. Lefferts. Comparative study of steam reforming of

methane, ethane and ethylene on Pt, Rh and Pd supported on yttrium-stabilized zirconia. *Applied Catalysis A: General*, Volume 332, Issue 2, 2007, Pages 310-317.

[11] V.V. Galvita, G.L. Semin, V.D. Belyaev, V.A. Semikolenov, P. Tsiakaras, and V.A. Sobyanin. Synthesis gas production by steam reforming of ethanol. *Applied Catalysis A: General*, Volume 220, Issues 1-2, 2001, Pages 123-127.

[12] K. Essaki, T. Muramatsu, and M. Kato. Effect of equilibrium-shift in the case of using lithium silicate pellets in ethanol steam reforming. *International Journal of Hydrogen Energy*, Volume 33, Issue 22, 2008, Pages 6612-6618.

[13] B. Silberova, H.J. Venvik, and A. Holmen. Production of hydrogen by short contact time partial oxidation and oxidative steam reforming of propane. *Catalysis Today*, Volume 99, Issues 1-2, 2005, Pages 69-76.

[14] G. Jones, J.G. Jakobsen, S.S. Shim, J. Kleis, M.P. Andersson, J. Rossmeisl, F. Abild-Pedersen, T. Bligaard, S. Helveg, B. Hinnemann, J.R. Rostrup-Nielsen, I. Chorkendorff, J. Sehested, and J.K. Nørskov. First principles calculations and experimental insight into methane steam reforming over transition metal catalysts. *Journal of Catalysis*, Volume 259, Issue 1, 2008, Pages 147-160.

[15] M.D. Falco. Pd-based membrane steam reformers: A simulation study of reactor performance. *International Journal of Hydrogen Energy*, Volume 33, Issue 12, 2008, Pages 3036-3040.

[16] K. Faungnawakij, R. Kikuchi, and K. Eguchi. Thermodynamic evaluation of methanol steam reforming for hydrogen production. *Journal of Power Sources*, Volume 161, Issue 1, 2006, Pages 87-94.

[17] Y. Matsumura and T. Nakamori. Steam reforming of methane over nickel catalysts at low reaction temperature. *Applied Catalysis A: General*, Volume 258, Issue 1, 2004, Pages 107-114.

[18] J.W.C. Liberatori, R.U. Ribeiro, D. Zanchet, F.B. Noronha, and J.M.C. Bueno. Steam reforming of ethanol on supported nickel catalysts. *Applied Catalysis A: General*, Volume 327, Issue 2, 2007, Pages 197-204.

[19] N. Laosiripojana, S. Assabumrungrat, and S. Charojrochkul. Steam reforming of ethanol with co-fed oxygen and hydrogen over Ni on high surface area ceria support. *Applied Catalysis A: General*, Volume 327, Issue 2, 2007, Pages 180-188.

[20] U. Hennings and R. Reimert. Stability of rhodium catalysts supported on gadolinium doped ceria under steam reforming conditions. *Applied Catalysis A: General*, Volume 337, Issue 1, 2008, Pages 1-9.

[21] A. Perna. Hydrogen from ethanol: Theoretical optimization of a PEMFC system integrated with a steam reforming processor. *International Journal of Hydrogen Energy*, Volume 32, Issue 12, 2007, Pages 1811-1819.

[22] E. Nikolla, J.W. Schwank, and S. Linic. Hydrocarbon steam reforming on Ni alloys at solid oxide fuel cell operating conditions. *Catalysis Today*, Volume 136, Issues 3-4, 2008, Pages 243-248.

[23] C.-H. Fu and J.C.S. Wu. A transient study of double-jacketed membrane reactor via methanol steam reforming. *International Journal of Hydrogen Energy*, Volume 33, Issue 24, 2008, Pages 7435-7443.

[24] K. Tomishige, M. Nurunnabi, K. Maruyama, and K. Kunimori. Effect of oxygen addition to steam and dry reforming of methane on bed temperature profile over Pt and Ni catalysts. *Fuel Processing Technology*, Volume 85, Issues 8-10, 2004, Pages 1103-1120.

[25] M. Kawano, T. Matsui, R. Kikuchi, H. Yoshida, T. Inagaki, and K. Eguchi. Steam reforming on Ni-samaria-doped ceria cermet anode for practical size solid oxide fuel cell at intermediate temperatures. *Journal of Power Sources*, Volume 182, Issue 2, 2008, Pages 496-502.

[26] A. Kundu, J.M. Park, J.E. Ahn, S.S. Park, Y.G. Shul, and H.S. Han. Micro-channel reactor for steam reforming of methanol. *Fuel*, Volume 86, Issue 9, 2007, Pages 1331-1336.

[27] J.P. Breen, R. Burch, and H.M. Coleman. Metal-catalysed steam reforming of ethanol in the production of hydrogen for fuel cell applications. *Applied Catalysis B: Environmental*, Volume 39, Issue 1, 2002, Pages 65-74.
[28] A. Houteit, H. Mahzoul, P. Ehrburger, P. Bernhardt, P. Légaré, and F. Garin. Production of hydrogen by steam reforming of methanol over copper-based catalysts: The effect of cesium doping. *Applied Catalysis A: General*, Volume 306, 2006, Pages 22-28.
[29] G. Manzolini and S. Tosti. Hydrogen production from ethanol steam reforming: Energy efficiency analysis of traditional and membrane processes. *International Journal of Hydrogen Energy*, Volume 33, Issue 20, 2008, Pages 5571-5582.
[30] A. Tugnoli, G. Landucci, and V. Cozzani. Sustainability assessment of hydrogen production by steam reforming. *International Journal of Hydrogen Energy*, Volume 33, Issue 16, 2008, Pages 4345-4357.
[31] J.-S. Suh, M.-T. Lee, R. Greif, and C.P. Grigoropoulos. A study of steam methanol reforming in a microreactor. *Journal of Power Sources*, Volume 173, Issue 1, 2007, Pages 458-466.
[32] S.R. Samms and R.F. Savinell. Kinetics of methanol-steam reformation in an internal reforming fuel cell. *Journal of Power Sources*, Volume 112, Issue 1, 2002, Pages 13-29.
[33] A. Casanovas, C.D. Leitenburg, A. Trovarelli, and J. Llorca. Catalytic monoliths for ethanol steam reforming. *Catalysis Today*, Volume 138, Issues 3-4, 2008, Pages 187-192.
[34] A. Bottino, A. Comite, G. Capannelli, R.D. Felice, and P. Pinacci. Steam reforming of methane in equilibrium membrane reactors for integration in power cycles. *Catalysis Today*, Volume 118, Issues 1-2, 2006, Pages 214-222.
[35] C. Cao, Y. Wang, and R.T. Rozmiarek. Heterogeneous reactor model for steam reforming of methane in a microchannel reactor with microstructured catalysts. *Catalysis Today*, Volume 110, Issues 1-2, 2005, Pages 92-97.
[36] C. Pistonesi, A. Juan, B. Irigoyen, and N. Amadeo. Theoretical and experimental study of methane steam reforming reactions over nickel catalyst. *Applied Surface Science*, Volume 253, Issue 9, 2007, Pages 4427-4437.
[37] Y. Mukainakano, K. Yoshida, S. Kado, K. Okumura, K. Kunimori, and K. Tomishige. Catalytic performance and characterization of Pt-Ni bimetallic catalysts for oxidative steam reforming of methane. *Chemical Engineering Science*, Volume 63, Issue 20, 2008, Pages 4891-4901.
[38] F. Gallucci, A. Basile, S. Tosti, A. Iulianelli, and E. Drioli. Methanol and ethanol steam reforming in membrane reactors: An experimental study. *International Journal of Hydrogen Energy*, Volume 32, Issue 9, 2007, Pages 1201-1210.
[39] A.P. Tsai and M. Yoshimura. Highly active quasicrystalline Al-Cu-Fe catalyst for steam reforming of methanol. *Applied Catalysis A: General*, Volume 214, Issue 2, 2001, Pages 237-241.
[40] K. Takeishi and H. Suzuki. Steam reforming of dimethyl ether. *Applied Catalysis A: General*, Volume 260, Issue 1, 2004, Pages 111-117.
[41] K. Essaki, T. Muramatsu, and M. Kato. Effect of equilibrium shift by using lithium silicate pellets in methane steam reforming. *International Journal of Hydrogen Energy*, Volume 33, Issue 17, 2008, Pages 4555-4559.
[42] S. Patel and K.K. Pant. Experimental study and mechanistic kinetic modeling for selective production of hydrogen via catalytic steam reforming of methanol. *Chemical Engineering Science*, Volume 62, Issues 18-20, 2007, Pages 5425-5435.
[43] L.L. Makarshin, D.V. Andreev, A.G. Gribovskiy, and V.N. Parmon. Influence of the microchannel plates design on the efficiency of the methanol steam reforming in microreactors. *International Journal of Hydrogen Energy*, Volume 32, Issue 16, 2007, Pages 3864-3869.
[44] D.K. Liguras, D.I. Kondarides, and X.E. Verykios. Production of hydrogen for fuel cells by steam

reforming of ethanol over supported noble metal catalysts. *Applied Catalysis B: Environmental*, Volume 43, Issue 4, 2003, Pages 345-354.

[45] F.C. Campos-Skrobot, R.C.P. Rizzo-Domingues, N.R.C. Fernandes-Machado, and M.P. Cantão. Novel zeolite-supported rhodium catalysts for ethanol steam reforming. *Journal of Power Sources*, Volume 183, Issue 2, 2008, Pages 713-716.

[46] K.S. Patel and A.K. Sunol. Modeling and simulation of methane steam reforming in a thermally coupled membrane reactor. *International Journal of Hydrogen Energy*, Volume 32, Issue 13, 2007, Pages 2344-2358.

[47] W. Yu, T. Ohmori, S. Kataoka, T. Yamamoto, A. Endo, M. Nakaiwa, and N. Itoh. A comparative simulation study of methane steam reforming in a porous ceramic membrane reactor using nitrogen and steam as sweep gases. *International Journal of Hydrogen Energy*, Volume 33, Issue 2, 2008, Pages 685-692.

[48] A.P. Kagyrmanova, I.A. Zolotarskii, E.I. Smirnov, and N.V. Vernikovskaya. Optimum dimensions of shaped steam reforming catalysts. *Chemical Engineering Journal*, Volume 134, Issues 1-3, 2007, Pages 228-234.

[49] M.D. Falco, L.D. Paola, and L. Marrelli. Heat transfer and hydrogen permeability in modelling industrial membrane reactors for methane steam reforming. *International Journal of Hydrogen Energy*, Volume 32, Issue 14, 2007, Pages 2902-2913.

[50] S. Grevskott, T. Rusten, M. Hillestad, E. Edwin, and O. Olsvik. Modelling and simulation of a steam reforming tube with furnace. *Chemical Engineering Science*, Volume 56, Issue 2, 2001, Pages 597-603.

[51] T. Valdés-Solís, G. Marbán, and A.B. Fuertes. Nanosized catalysts for the production of hydrogen by methanol steam reforming. *Catalysis Today*, Volume 116, Issue 3, 2006, Pages 354-360.

[52] J.-H. Ryu, K.-Y. Lee, H. La, H.-J. Kim, J.-I. Yang, and H. Jung. Ni catalyst wash-coated on metal monolith with enhanced heat-transfer capability for steam reforming. *Journal of Power Sources*, Volume 171, Issue 2, 2007, Pages 499-505.

[53] A.L.Y. Tonkovich, B. Yang, S.T. Perry, S.P. Fitzgerald, and Y. Wang. From seconds to milliseconds to microseconds through tailored microchannel reactor design of a steam methane reformer. *Catalysis Today*, Volume 120, Issue 1, 2007, Pages 21-29.

[54] A.Y. Tonkovich, S. Perry, Y. Wang, D. Qiu, T. LaPlante, and W.A. Rogers. Microchannel process technology for compact methane steam reforming. *Chemical Engineering Science*, Volume 59, Issues 22-23, 2004, Pages 4819-4824.

[55] N. Iwasa, T. Mayanagi, W. Nomura, M. Arai, and N. Takezawa. Effect of Zn addition to supported Pd catalysts in the steam reforming of methanol. *Applied Catalysis A: General*, Volume 248, Issues 1-2, 2003, Pages 153-160.

[56] R. Peters, R. Dahl, U. Klüttgen, C. Palm, and D. Stolten. Internal reforming of methane in solid oxide fuel cell systems. *Journal of Power Sources*, Volume 106, Issues 1-2, 2002, Pages 238-244.

[57] A.P. Simpson and A.E. Lutz. Exergy analysis of hydrogen production via steam methane reforming. *International Journal of Hydrogen Energy*, Volume 32, Issue 18, 2007, Pages 4811-4820.

[58] J. Sehested. Four challenges for nickel steam-reforming catalysts. *Catalysis Today*, Volume 111, Issues 1-2, 2006, Pages 103-110.

[59] W. Yu, T. Ohmori, T. Yamamoto, A. Endo, M. Nakaiwa, and N. Itoh. Optimal design and operation of methane steam reforming in a porous ceramic membrane reactor for hydrogen production. *Chemical Engineering Science*, Volume 62, Issues 18-20, 2007, Pages 5627-5631.

[60] K. Faungnawakij, R. Kikuchi, and K. Eguchi. Thermodynamic analysis of carbon formation boundary and reforming performance for steam reforming of dimethyl ether. *Journal of Power Sources*, Volume 164, Issue 1, 2007, Pages 73-79.

[61] G. Rabenstein and V. Hacker. Hydrogen for fuel cells from ethanol by steam-reforming, partial-oxidation and combined auto-thermal reforming: A thermodynamic analysis. *Journal of Power Sources*, Volume 185, Issue 2, 2008, Pages 1293-1304.

[62] P.A. Erickson. Statistical validation and an empirical model of hydrogen production enhancement found by utilizing a controlled acoustic field in the steam-reforming process. *International Journal of Hydrogen Energy*, Volume 31, Issue 12, 2006, Pages 1690-1697.

[63] T.A. Semelsberger and R.L. Borup. Thermodynamic equilibrium calculations of dimethyl ether steam reforming and dimethyl ether hydrolysis. *Journal of Power Sources*, Volume 152, 2005, Pages 87-96.

[64] S. Rakass, H. Oudghiri-Hassani, P. Rowntree, and N. Abatzoglou. Steam reforming of methane over unsupported nickel catalysts. *Journal of Power Sources*, Volume 158, Issue 1, 2006, Pages 485-496.

[65] B.P. Ngoc, C. Geantet, M. Aouine, G. Bergeret, S. Raffy, and S. Marlin. Quasicrystal derived catalyst for steam reforming of methanol. *International Journal of Hydrogen Energy*, Volume 33, Issue 3, 2008, Pages 1000-1007.

[66] D.L. Trimm. Coke formation and minimisation during steam reforming reactions. *Catalysis Today*, Volume 37, Issue 3, 1997, Pages 233-238.